Atmos. Chem. Phys. Discuss., 11, 28061–28095, 2011
www.atmos-chem-phys-discuss.net/11/28061/2011/
doi:10.5194/acpd-11-28061-2011

Atmospheric Chemistry and Physics Discussions

Enhancement and depletion of lower/middle tropospheric ozone in Senegal during pre-monsoon and monsoon periods of summer 2008: observations and model results

G. S. Jenkins[1], S. Ndiaye[2], M. Gueye[2], R. Fitzhugh[3,*], J. W. Smith[1], and A. Kebe[4]

[1]Howard University Program in Atmospheric Science, Washington DC 20059, USA
[2]Lab for Atmospheric-Oceanic Physics-Simeon Fongang, Cheikh Anta Diop University, Dakar, Senegal
[3]Department of Atmospheric Ocean and Space Science, University of Michigan, Ann Arbor, Michigan, USA
[4]Senegal Meteorological Agency, Dakar, Senegal
[*]now at: ITT Corporation 1447 St. Paul Rochester, NY 14621, USA

Received: 21 September 2011 – Accepted: 3 October 2011 – Published: 19 October 2011

Correspondence to: G. S. Jenkins (gjenkins@howard.edu)

Published by Copernicus Publications on behalf of the European Geosciences Union.

ACPD
11, 28061–28095, 2011

Abstract

During the summer (8 June through 3 September) of 2008, 9 ozonesondes are launched from Dakar, Senegal (14.75° N, 17.49° W) to investigate ozone (O_3) variability in the lower/middle troposphere during the pre-monsoon and monsoon periods. Results during June 2008 (pre-monsoon period) show a reduction in O_3 concentrations, especially in the 850–700 hPa layer with Saharan Air Layer (SAL) events. However, O_3 concentrations are increased in the 950–900 hPa layer where the peak of the inversion is found and presumably the highest dust concentrations. We also use the WRF-CHEM model to gain greater insights for observations of elevated/reduced O_3 concentrations during the pre-monsoon/monsoon periods. In the transition period between 26 June and 2 July in the lower troposphere (925–600 hPa), a significant increase in O_3 concentrations occur which we suggest is caused by enhanced biogenic NO_x emissions from Sahelian soils following rain events on 28 June and 1 July. During July and August 2008 (monsoon period), with the exception of one SAL outbreak, vertical profiles of O_3 are well mixed with concentrations not exceeding 55 ppb between the surface and 550 hPa. The results suggest that during the pre-monsoon period ozone concentrations in the lower troposphere are controlled by the SAL, which destroys ozone through heterogeneous processes. At the base of the SAL we also find elevated levels of ozone, which we attribute to biogenic sources of NO_x from Saharan dust that are released in the presence of moist conditions. Once the monsoon period commences, wet and dry deposition become important sinks of ozone in the Sahel with episodes of ozone poor air that is horizontally transported from low latitudes into the Sahel. These results support aircraft chemical measurements and chemical modeling results from the African Monsoon Multidisciplinary Analysis (AMMA) field campaign.

ACPD
11, 28061–28095, 2011

1 Introduction

Mean tropospheric ozone (O_3) concentrations in the tropics are controlled by biomass burning, lightning, biogenic and anthropogenic emissions, which act as sources of ozone while deposition and heterogeneous chemistry, act as sinks of ozone. Because tropospheric ozone impacts the oxidizing capacity of the atmosphere and is a greenhouse gas with positive radiative forcing contributing to global warming, it is important to quantify the various ozone sinks, sources and variability. Tropospheric ozone balloon measurements are made on a regular basis on most land areas around the globe, except in Africa; however, ozone measurements are made in Southern Africa on a regular basis as part of the SHADOZ network (Thompson et al., 2003). Recently, two years of regular ozone measurements were made in West Africa at Cotonou, Benin (6.21° N, 2.23° E) where biomass burning during the Northern Hemisphere (NH) winter season occurs on an annual basis elevating ozone in the lower troposphere (Thouret et al., 2009). The measurements at Cotonou, Benin also show the influence of biomass burning from the Southern Hemisphere (SH) during NH summer, which elevate ozone concentrations in the lower troposphere (Real et al., 2010). Further north, in the Sahelian region, seven ozonesondes were launched in Senegal (14.6° N, 17.1° W) between 30 August and 16 September 2006 showing the vertical transport of ozone from the middle/upper troposphere to the lower troposphere by convective downdrafts in mesoscale convective systems (Grant et al., 2008).

Because the Sahel is further north and under the influence of biomass burning primarily during the NH winter but not during NH summer, it is not definitive what drives tropospheric ozone variability on a daily, weekly or monthly basis during the NH summer season. A likely source of NH summer season tropospheric ozone variability is associated with the Saharan Air Layer (SAL) and dust emissions. Each year, between May and October, the SAL (Carlson and Prospero, 1972; Dunion and Veldon, 2004) is an important meteorological feature influencing continental areas of West Africa and the Northern Tropical Atlantic. The SAL is characterized by dry (low relative humidity),

ACPD
11, 28061–28095, 2011

stable air (an inversion capped above the marine boundary layer), a mid-level easterly jet and reduced visibilities from enhanced dust. Annual dust emissions from Africa range from 160–1600 Tg yr^{-1} with major sources of surface dust emissions in Mauritania, Mali and Algeria during June–July and August (Engelstaedter et al., 2006; Middleton and Goudie, 2001).

A number of observational studies have shown reduced ozone concentrations in the presence of Saharan dust (De Reus et al., 2000; Bonasoni et al., 2004). The desert aerosols can reduce tropospheric O_3 concentrations at a single location in multiple ways: (a) dust aerosols may serve as deposition sites for O_3 while also reducing photolysis rates (Bian and Zender, 2003; De Reus et al., 2000). (b) Heterogeneous chemistry on aerosol surfaces can reduce important precursors (OH, HO_2) associated with O_3 production (Zhang et al., 1994; Bian and Zender, 2003; Tang et al., 2003). (c) The production of Nitric Acid (HNO_3), leading to particulate nitrate can act as a sink for NO_x and limit O_3 production (Zhang et al., 1994; Jacob, 2000; De Reus et al., 2000; Tang et al., 2003). Hence, the SAL and its dust emissions can act as a potential sink for ozone, reducing its positive greenhouse forcing while also scattering solar radiation causing daytime cooling at the surface. Recent observations of the SAL have examined its radiative impact (Myhre et al., 2003), chemical composition (Twohy et al., 2008), aerosol and water vapor structure (Ismail et al., 2010), and potential impact on African Easterly Waves (AEWs) and Tropical Cyclogenesis (Jenkins et al., 2008a; Zipser et al., 2009).

As the NH summer season evolves, there are additional sources and sinks that can influence O_3 concentrations in the lower troposphere. The sources include: biogenic NO_x at the start of the wet season and the vertical transport of ozone from the middle/upper troposphere associated with lightning and convective downdrafts (Grant et al., 2008). Wet/dry deposition and the transport of ozone poor air from equatorial regions should become the primary reason for lower ozone concentrations during the wet season.

ACPD
11, 28061–28095, 2011

Satellite and aircraft observations along with modeling studies have identified NO_x emissions from soil as an important source of tropospheric NO_x during June, July and August in Sahelian and Saharan zones (Jeagle et al., 2004; Van der A et al., 2008; Williams et al., 2009; Delon et al., 2008, 2010). Pulses of biogenic NO_x emissions are released into the atmosphere from the soil at the end of the dry season with the first rains. During the 2006 African Monsoon Multidisciplinary Analyses (AMMA) campaign (Redelsperger et al., 2006), aircraft measurements flown over wet/dry soils show higher NO_x concentrations in the boundary layer over recently wet soils (Stewart et al., 2008). O_3 concentrations are significantly higher over wet soils than dry soils and low correlations with CO imply that NO_x production is not associated with anthropogenic or biomass burning sources (Stewart et al., 2008). A sharp gradient in O_3 concentrations are found implying locally produced O_3 estimated at 1 ppb h^{-1} from soil NO_x.

Deposition serves as a primary sink of ozone and a reduction in O_3 concentrations during the monsoon period and is expected because of increased deposition with the rapid growth of vegetation beginning with the start of the wet season. After June, the northward movement of the monsoon and the accompanying southwest moist flow leads to increased instability and precipitation. The precipitation supplies an important source of moisture for vegetation growth in West Africa (Guinea and Sahelian regions). The expansion of vegetation leads to increased deposition and a north-south gradient in deposition rates and hence ozone concentrations in the lower troposphere. Measurements in Senegal during 2006 estimate a maximum deposition velocity of 1.5 cm s^{-1} with higher values noted during precipitation events (Grant et al., 2008). The removal of NO_x through wet deposition would lead to further reductions in O_3 concentrations in lower latitudes relative to the drier semi-arid and arid regions in the Sahelian Zone and Sahara desert (Delon et al., 2010). The north-south gradient (with maximum ozone concentrations at 16° N) in lower tropospheric (below 900 hPa) ozone concentrations is found during July and August 2006 by Reeves et al. (2010) which is related to vegetation cover, and deposition. A north-south gradient in NO_x is also found with the maximum values found between 13–16° N which Reeves et al. (2010) attribute to biogenic

ACPD
11, 28061–28095, 2011

emissions of NO_x from soils after precipitation events.

Moreover, northward surges in the monsoon flow or the passage of 3 to 5 day AEWs (Burpee, 1972) should lead to an overall poleward transport of ozone poor air in the lower troposphere, because of more vegetation and higher deposition rates in lower latitudes; onshore flow from the Atlantic ocean would also transport in ozone poor air. Conversely surges of dry air from desert regions should lead to an equatorward transport of ozone-enriched air to lower latitudes.

The specific objectives of this paper are: (1) to examine the variability of O_3 concentrations in the lower/middle troposphere, with an emphasis on the 925–550 hPa layer during the dry (pre-monsoon) and wet periods (monsoon) in the Sahelian Zone (Dakar, Senegal); (2) to quantify the influence of the SAL and AEWs on O_3 concentrations in the 925–550 hPa layer; (3) to determine if the impacts of early rains enhance O_3 concentrations in the lower troposphere because of the release of biogenic NO_x.

2 Observational data and model simulations

In preparation for ozonesonde launches Vaisala ECC6AB ozonesondes are prepared 3–7 days in advance and launched in concert with RS92 radiosonde at 12:00 UTC during June, July and August of 2008. Table 1 shows the 9 ozonesonde launches from Dakar, Senegal (14.75° N, 17.49° W) during the period. Average ozone profiles for SAL, non-SAL and all ozone profiles are produced by averaging vertically over 10 hPa layers from the surface through 450 hPa. Aerosol observations in the form of Aerosol Optical Thickness (AOT) are produced from the Aerosol Robotic Network (AERONET) at Mbour, Senegal (14.39° N, 16.59° W) and from the Space-borne Ozone Monitoring Instrument (OMI) Aerosol Index (AI) for the summer of 2008. The $1^\circ \times 1^\circ$ Deep Blue product from the Moderate Resolution Imaging Spectrometer (MODIS) instrument aboard the AQUA satellite is used for AOT over land areas. Daily averages of AOT are constructed from the hourly AOT data from Mbour, Senegal. Monthly satellite estimates of Tropospheric Column Ozone (TCO) for the summer of 2008 at $1^\circ \times 1.25^\circ$ are also used to examine spatial and temporal patterns of ozone (Ziemke et al., 2006).

ACPD
11, 28061–28095, 2011

To address daily and seasonal tropospheric O_3 variations for comparison with the ozonsonde measurements the Weather and Research Forecasting with Chemistry (WRF-CHEM) model is used to simulate O_3 concentrations over West Africa during the summer of 2008 (Grell et al., 2005). The WRF-CHEM computes gas phase chemistry with 55 prognostic species and 134 reactions (Fast et al., 2005). The WRF-CHEM simulations use 30 km grid spacing, 27 vertical levels and the top of the model is 50 hPa. The biogenic sources of volatile organic compounds are computed (Guenther et al., 1995) and the model is initialized from a uniform state with O_3 concentrations increasing with height to the stratosphere. NCEP final analyses at 6-h intervals provide meteorological initial and boundary conditions to the WRF-CHEM. Here we define the pre-monsoon period as the month of June and the monsoon period from July through September.

3 Results

3.1 Summer overview for 2008

Figure 1a–d shows the satellite derived TCO values across West Africa and the Eastern Atlantic for June through September of 2008. A north-south gradient of TCO values with higher values are found over the Sahara relative to Sahelian and Guinean regions of West Africa. The north-south TCO gradient is weakest and strongest during June and August, respectively. During June, TCO values of 37–40 DU are found over the desert regions with slightly lower values to the south (Fig. 1a). However, by August TCO values are considerably lower over the Sahelian and Guinea regions of West Africa and can be attributed to dry/wet deposition. Figure 2a–c shows the OMI AI along with the AOT from Mbour, Senegal for the period of ozonesonde launches during 2008. There are a number of high AI/AOT days associated with SAL outbreaks during June and July and considerably fewer days in August. There are 5 days when the AI is greater than 2.5 during June, 3 days in July and 1 day in August, respectively. There

ACPD
11, 28061–28095, 2011

are 7 days with the AOT is greater than 0.6 in June, 4 days in July and 2 days in August, respectively. The OMI AI is positively correlated to the Mbour AOT values with correlations of 0.82, 0.86 and 0.79 during June, July and August, respectively. TRMM daily averaged rain amounts for a 5° × 5° box (11.5–16.5° N, 12.5–17.5° W) over Senegal and Gambia show very little precipitation until the end of June when wetter conditions begin and continue through July and August (Fig. 2d).

Figure 3a shows the vertical profiles of relative humidity (RH) for SAL, non-SAL and the average of all 9 ozonesondes. The SAL profile is considerably drier above 950 hPa with the minimum average RH values of approximately 15–20 % between 925 and 900 hPa. For mean non-SAL conditions, the relative humidity is approximately 70 % in the 925–550 hPa layer. Corresponding to the dry air associated with the SAL are lower ozone concentrations in the 925–550 hPa layer (Fig. 3b). The largest differences of 10–14 ppb are found near 850 hPa and 600 hPa, respectively. The mean results are in agreement with the earlier results of De Reus et al. (2000) and Bonasoni et al. (2004) showing ozone reductions associated with the SAL and aerosol loading. Table 1 shows that highest column ozone in the 925–550 hPa layer is found on 12 June (20.5 DU). The lowest column ozone in the 925–550 hPa layer is found on 27 September (6.4 DU) followed by 8 June (6.6 DU). Only small differences in the average 925–550 hPa O_3 column are found between the pre-monsoon period (11.3 DU) and the monsoon period (10.5 DU). Larger differences in the average 925–550 hPa O_3 column and relative humidity are found for SAL (9.2 DU, 33.3 %) versus non-SAL conditions (13 DU, 72.4 %). We define SAL conditions where dry, stable air is found in the 925–550 hPa layer. Next we look in greater detail at individual ozonesonde launches during the pre-monsoon and monsoon periods.

3.2 Pre-monsoon O_3 measurements

There are 3 ozonesonde launches, 8, 10, 15 June with OMI AI values > 2 and low relative humidity (Table 1) which are associated with SAL events in Fig. 2. During the pre-monsoon period (Fig. 4a), low O_3 concentrations (< 20 ppb) are found on 8 and

ACPD
11, 28061–28095, 2011

10 June relative to the other profiles, especially in the 850–600 hPa layer. These two days have the lowest 925–550 hPa column ozone values during the pre-monsoon period (Table 1). At the base of the SAL (950–900 hPa layer), there is also evidence of enhanced O_3 concentrations on 8, 10 June in Fig. 4a. Figure 4b shows low relative humidity (< 20 %) at approximately 950 hPa for 8, 10, 12 and 15 June, which begins to increase at pressure levels less than 700 hPa, except for 12 June where RH values rapidly increase above 900 hPa. Figure 4c shows that a temperature inversion is present for all pre-monsoon ozone profiles, but the strongest temperature inversions are found for 8, 10 and 15 June. It is at the peak of the temperature inversion that increases in O_3 concentrations are found (Fig. 4a). This is also the altitude where high dust concentrations are found (Ismail et al., 2010).

Figure 5a–h shows OMI-AI with 925 hPa streamlines along with the Deep Blue AOT overlain by 700 hPa streamlines for identifying dust and AEWs during the pre-monsoon period. Elevated aerosol loadings on 8, 10 and 15 June are associated with either northerly or northeasterly winds at 925 hPa (Fig. 5a, b, d). In contrast, winds with a southerly component are found on 12 June and 26 June (Fig. 5c, e). Moreover an African Easterly Wave (AEW) as viewed with 700 hPa streamlines, exits the continent on 12 June and is associated with elevated RH, cloudiness and precipitation in Dakar. Reduced O_3 concentrations between 850 and 600 hPa on 8, 10 June in concert with higher AI/AOT from Saharan dust support ozone reduction through heterogeneous interactions between dust and gas-phase chemistry (De Reus et al., 2000).

3.3 Pre-monsoon/monsoon transition

As shown in Fig. 2d, an upward trend in daily rain amounts occurs in late June as the pre-monsoon period transitions to the monsoon period. Figure 3b shows that O_3 concentrations between 950 and 600 hPa are considerably higher at the start of the monsoon period (2 July) when compared to the end of the pre-monsoon period (26 June). O_3 concentrations are 10–20 ppb larger on 2 July when compared to 26 June. The enhancement of O_3 concentrations coincides with several rainfall events in Senegal

ACPD
11, 28061–28095, 2011

in the vicinity of Dakar on 28, 30 June (Fig. 6a, b). TRMM daily rain estimates are highest on 1 July with daily amount approaching 80 mm in some areas to the east of Dakar (Fig. 6d). The rainfall is associated with the passage of an AEW on 1 July and a plausible cause for ozone enhancement between 26 June and 2 July by biogenic NO_x emissions from wet Sahelian soils. The measured enhanced O_3 concentrations between 26 June and 2 July are consistent with the ozone enhancement via biogenic NO_x pulses in soils from the observations of Stewart et al. (2008).

3.4 Monsoon O_3 measurements

During the monsoon period, the vertical profiles of O_3 concentrations slowly increase for, 27 August and 3 September launches in the surface-550 hPa layer; a decrease in O_3 concentrations is found above 850 hPa on 2 July (Fig. 7a). Well-mixed O_3 profiles were observed in Senegal during the monsoon period (late August through mid-September) of 2006 (Grant et al., 2008). The 2 August measurement shows the enhance/depletion pattern of O_3 concentrations in the vertical profile as in earlier pre-monsoon SAL events; an ozone enhancement near the peak of the SAL temperature inversion and reduced O_3 concentrations is found immediately above this level (Fig. 7a). Profiles of RH in Fig. 7b shows humid conditions over Senegal during July, August and September except for 2 August when a SAL event occurs over Senegal. The 2 August vertical profile of RH shows values less than 10 % in the 950–900 hPa layer. In contrast, a very moist profile can be found on 27 August with RH values between 90 and 100 % from 950 through 750 hPa. A large temperature inversion is found on 2 August in association with the SAL event with smaller temperature inversions found in the other three monsoon measurements (Fig. 7c). Table 1 shows that during the monsoon period the lowest column O_3 is found on 27 August in association with the highest relative humidity values in the 925–550 hPa layer.

Figure 8a–h shows OMI AI with 925 hPa streamlines along with the Deep Blue AOT overlain by 700 hPa streamlines for identifying dust and AEWs for the launch dates during the monsoon period. During this period, only 2 August shows elevated AI and

ACPD
11, 28061–28095, 2011

AOT in association with a thermal low (heat low) over Southern Mauritania (Fig. 8b). During the other three days (2 July, 27 August, 3 September), the highest AI or AOT values are found over higher latitudes (> 20°). Also evident at 700 hPa are strong AEWs, which have closed vortices on 2 July, 27 August and 3 September (Fig. 8e, g, h). The AEWs on 2 July and 27 August are associated with Tropical Cyclones Bertha and Ike, respectively (Rhome, 2008; Berg, 2008).

3.5 WRF-CHEM simulations of elevated O_3 concentrations on 12 June and reduced O_3 concentrations during the monsoon period

Table 1 shows that during the period of 10 June through 12 June, the 925–550 hPa column O_3 values are increased by a factor of 2.77, between the SAL air mass and the passage of the AEW. This is followed by a decreased in 925–550 hPa column O_3 values by a factor of 1.8 between 12 and 15 June. The elevated O_3 concentrations on 12 June could be due to: (a) a stratospheric intrusion; (b) a biogenic pulse of NO_x from Sahelian soils enhancing O_3 concentrations or; (c) lightning-NO_x which enhances O_3 concentrations that is then transported to the lower/middle troposphere (Grant et al., 2008). To address a possible stratospheric influence, the WRF-CHEM is initialized at four different times at 00:00 UTC, 1 June; 12:00 UTC, 4 June; 12:00 UTC 5 June; 12:00 UTC 6 June to simulate elevated O_3 concentration for the period of 10–12 June. Figure 9a–d shows for the period of 8 June and 13 June that higher concentrations of O_3 are found in the middle and upper troposphere based on vertical profiles of O_3 at 14.5° N, 17.5° W near Dakar, Senegal, in a region of weak sinking motion. WRF-CHEM forecasts that are initialized on 5 and 6 June show O_3 concentrations in the 90 to 120 ppb range at the 200–300 hPa levels with values of 35–50 ppb extending downward into the middle troposphere (Fig. 9c, d).

The simulated enhancement of upper tropospheric ozone is consistent with the observations between 10 and 12 June where a significant increase in ozone concentrations is found. Figure 10a provides further support for a stratospheric intrusion when comparing the observed ozone concentrations on 10, 12 June for 1000–150 hPa

ACPD
11, 28061–28095, 2011

levels. On 12 June observed O_3 concentrations in the range of 75–100 ppb are found in the 400–250 hPa layer. However, O_3 concentrations dramatically increase from 142–443 ppb between 242 hPa and 226 hPa with O_3 concentrations remaining above 100 ppb through 210 hPa. Figure 10b shows the simulated vertical profile of ozone concentrations on 9 and 11 June at 12:00 UTC at 14.75° N, 17.5° W (near Dakar) based on a 6 June 1200 WRF-Chem initialization. 11 June is used because the simulated AEW arrives to Dakar one day before observations suggest. The largest differences in ozone concentrations are found above 400 hPa where increase of 30 ppb is found at 250 hPa between 9 and 11 June. While the enhancement in simulated O_3 concentrations is smaller than observed, they do support a stratospheric influence in the upper troposphere above Dakar during the period of 10–12 June 2008. Smaller simulated increases of O_3 concentrations are found in the SAL layer (925–550 hPa), on the order of 10 ppb, which is much smaller than the observed values (Fig. 10a).

Figure 10c shows significant differences for the observed average (over 10 hPa layers) O_3 concentrations for 10, 12 and 15 June. O_3 concentrations are nearly 40 ppb larger on 12 June relative to 10 June near 800 and 550 hPa; O_3 concentrations are approximately 20 ppb larger on 12 June relative to 15 June near 800 and 550 hPa. While there may be some O_3 enhancement in the lower to middle troposphere by vertical transport from the upper troposphere, it is equally plausible that the large observed changes in lower/middle tropospheric ozone concentrations between 10 and 12 June are associated with multiple factors. These factors include: ozone destruction, associated with heterogeneous chemistry, in the SAL layer on 10 June; lightning-NO_x leading to O_3 enhancement followed by downward vertical transport by convective downdrafts with the AEW; ozone enhancement via biogenic NO_x emissions released from wet soils to the south or east of Dakar. Figure 10d shows the largest amounts of precipitation falling in Southeastern Senegal on 12 January as the AEW moved eastward. Only minimal amounts of rain fell at Dakar and this occurred after the 12:00 UTC launch.

Next we use WRF-CHEM to explore the observed lower O_3 concentrations that are generally well mixed during August and September. Table 1 shows low 925–550 hPa

ACPD
11, 28061–28095, 2011

column O_3 under moist and low aerosol loading conditions. In particular, 27 August and 3 September measurements show low concentrations of O_3 that are well mixed relative to the 2 July O_3 measurements under humid conditions (Fig. 7a). There are several factors that could lead to well mixed, reduced O_3 concentrations in the monsoon season: (a) increased dry and wet deposition; and (b) the northward transport of O_3 poor air from areas to the south of the Sahel.

Measurements at Dakar, Senegal for 27 August, and 3 September suggest that one or both factors are responsible for low O_3 concentrations in the lower troposphere. In each case, very moist conditions with the 925 hPa flow coming from the Atlantic Ocean (Fig. 8c) and lower latitudes (Fig. 8d) are found with the approach or passage of an AEW at 700 hPa (Fig. 8g, h). The monthly averaged TCO values (Fig. 1) along with recent measurements during the AMMA field campaign support a north-south gradient in the lower troposphere with lower O_3 concentrations found in equatorward latitudes of West Africa (Saunois et al., 2008).

To examine simulated seasonal O_3 concentrations and its relationship to relative humidity we show WRF-CHEM forecasted 925 hPa 12-h instantaneous O_3 concentrations and relative humidity averaged over the area of 14–16° N and 18–16° W for June, July and August and early September (Fig. 11). The highest O_3 concentrations are found during the month of June with significant reductions simulated during the months of July and August. Simulated O_3 concentrations of 10–20 ppb are common at 925 hPa during the monsoon period (Fig. 11a). The lower simulated O_3 concentrations are found when the simulated relative humidity (RH) at 850 hPa begins to increase during the monsoon period (Fig. 11b). Elevated relative humidity at 850 hPa can be used as a proxy of the monsoon flow during July, August and September. The simulated increases in relative humidity are in agreement with satellite observed wetter conditions during July and August (Fig. 2d).

ACPD
11, 28061–28095, 2011

4 Discussion and summary

Results show that reductions of O_3 concentrations (10–15 ppb) in the lower troposphere are associated with SAL (Fig. 1). However, an examination of individual SAL ozonesonde profiles also show an increase in O_3 concentrations near the peak of the inversion. Figure 12a–d illustrates the vertical profiles of O_3 concentration, relative humidity and temperature in the 1000–750 hPa layer for the four SAL events that occurred during the summer of 2008. Similar vertical profiles of enhanced O_3 concentrations (> 50 ppb for 2 August) are found in three (8, 10 June, 2 August) of the four ozonesondes: an increase in O_3 concentrations, which overlaps a temperature inversion and very low relative humidity values near the base of the SAL (Fig. 12a, b, d). Above the layer where O_3 concentrations are enhanced, there is a reduced layer of O_3 concentrations in the 900–750 hPa layer. The layer of lower O_3 concentrations in the SAL layer in Fig. 12 is consistent with the earlier results of De Reus et al. (2000) and Bonasoni et al. (2004) with heterogeneous chemistry being a primary source of O_3 depletion (Zhang et al., 1994; Tang et al., 2004). Tang et al. (2004) show through modeling studies and aircraft observations that losses of O_3 and HNO_3 through direct interaction with dust were large during observed dust storms in the ACE-Asia field campaign.

Figure 13a depicts the changes in aerosol concentrations, relative humidity and O_3 concentrations, during an ideal SAL event with significant dust loading, based on the findings from this study. During this SAL event, a vertical profile of O_3 would show: layer A – from the surface to 950 hPa with slowly increasing O_3 concentrations and low aerosol concentrations; layer B – a 50–100 hPa layer with elevated O_3, high aerosols concentrations and a strong temperature inversion; layer C – a 100–200 hPa layer with reduced O_3 concentrations and smaller sized aerosols. One might expect the largest losses of O_3 in layer B in association with heterogeneous reactions but the observations show that this is not the case and the opposite is found, hence, there must be a source of O_3. The most likely source would be biogenic NO_x from Saharan soils that have been lifted that act as a source of atmospheric O_3 in downstream regions. The exact mechanism for O_3 enrichment near the base of the SAL remains uncertain.

ACPD
11, 28061–28095, 2011

A suggested mechanism for enhancing O_3 concentrations in this shallow layer may come from the activation of biogenic NO_x when encountering moist conditions (Fig. 13b). Nitrate formation on dust aerosols is an end product after heterogeneous reactions between HNO_3 and dust aerosols. Gravitational settling of aerosols between 900–600 hPa may lead to significant amounts of aerosols with nitrate on its surfaces through heterogeneous processes, which accumulate just above the inversion. At Dakar, very moist conditions (RH > 80 %) are found from the surface to the 950 hPa just below the inversion associated with the SAL. Even though the inversion inhibits vertical motions, some mixing between the SAL layer and the shallow moist layer below is possible.

Vlasenko et al. (2006) show in laboratory studies that nitrate-coated dust aerosols will increase their hygroscopicity in the presence of high relative humidity. Twohy et al. (2009) and Ismail et al. (2010) show that some SAL events have areas of enhanced moisture embedded within the SAL and that dust particles from the desert have hydroscopic properties and can serve as cloud condensation nuclei (CCN). Some critical threshold of moisture on the surface of the aerosols could lead water stressed microbes to denitrify and release airborne biogenic NO_x producing higher O_3 concentrations.

Other findings include:

– Elevated O_3 concentrations in the upper troposphere on 12 June are likely caused by a stratospheric intrusion based on WRF-CHEM results. In the lower to middle troposphere, the depletion of O_3 in the SAL layer on 10 June followed by an increase in O_3 concentrations with the passage of the AEW on 12 June seem to be responsible for the observed changes. Other mechanisms such as lightning-NO_x leading to O_3 enhancement followed by downward vertical transport by convective downdrafts associated with the AEW cannot be ruled out as an additional source of ozone enhancement in the middle/lower troposphere on 12 June (Jenkins et al., 2008b; Grant et al., 2008).

ACPD
11, 28061–28095, 2011

- During the transition between the pre-monsoon and monsoon periods (26 June and 2 July) a significant enhancement of O_3 concentrations in the lower/middle troposphere are found after precipitation events in areas surrounding Dakar on 28 June and 1 July 2008. We suggest that pulses of biogenic NO_x emissions from dry Sahelian soils are the primary cause of enhanced O_3 concentrations, which is consistent with earlier studies (Stewart et al., 2008; Delon et al., 2008, 2010; Reeves et al., 2010).

- Low O_3 concentrations are found in the 925–550 hPa layers during the monsoon period (27 August and 3 September) and likely linked to dry deposition and wet deposition during the monsoon period (Grant et al., 2008; Delon et al., 2010).

Our measurements suggest that the passage of the SAL and AEWs can lead to reductions of tropospheric O_3 in the lower/middle troposphere in the Sahelian Zone by heterogeneous chemistry and deposition based on measurements from Dakar. However, biogenic sources of NO_x may also enhance lower tropospheric O_3 in the Sahelian Zone. Additional chemical, radiative and aerosol measurements along with chemical modeling on a regional basis in West Africa will provide additional insights into the processes that control O_3 concentrations in the lower troposphere. During the summers of 2010 and 2011 high frequency O_3 measurements from Dakar during the pre-monsoon and monsoon periods are undertaken. These results should provide further evidence of O_3 variability associated with the SAL and AEWs.

Acknowledgements. This work was supported by The National Science Foundation (NSF) on project AGS-0621529. We thank all of the Met operators for their help in this project. We thank Didlier Tanre for their efforts in establishing and maintaining the Mbour, Senegal site.

ACPD
11, 28061–28095, 2011

References

Berg, R.: Tropical Cyclone Report Hurricane Ike (AL092008), National Hurricane Center, available at: http://www.nhc.noaa.gov/2008atlan.shtml, 2008.

Bian, H. and Zender, C. S.: Mineral dust and global tropospheric chemistry: relative roles of photolysis and heterogeneous uptake, J. Geophys. Res., 108, 4672, doi:10.1029/2002JD003143, 2003.

Bonasoni, P., Cristofanelli, P., Calzolari, F., Bonafè, U., Evangelisti, F., Stohl, A., Zauli Sajani, S., van Dingenen, R., Colombo, T., and Balkanski, Y.: Aerosol-ozone correlations during dust transport episodes, Atmos. Chem. Phys., 4, 1201–1215, doi:10.5194/acp-4-1201-2004, 2004.

Burpee, R. W.: The origin and structure of easterly waves in the lower troposphere of North Africa, J. Atmos. Sci., 29, 77–90, 1972.

Carlson T. and Prospero, J. M.: The large-scale movement of Saharan air outbreaks over the Northern Equatorial Atlantic, J. Appl. Meteorol., 11, 283–297, 1972.

De Reus, M., Dentener, F., Thomas, A., Borrmann, S., Ström, J., and Lelieveld, J.: Airborne observations of dust aerosols over the North Atlantic during ACE2: Indications for heterogeneous ozone destruction, J. Geophys. Res., 105, 15263–15275, 2000.

Delon, C., Reeves, C. E., Stewart, D. J., Serça, D., Dupont, R., Mari, C., Chaboureau, J.-P., and Tulet, P.: Biogenic nitrogen oxide emissions from soils – impact on NO_x and ozone over West Africa during AMMA (African Monsoon Multidisciplinary Experiment): modelling study, Atmos. Chem. Phys., 8, 2351–2363, doi:10.5194/acp-8-2351-2008, 2008.

Delon, C., Galy-Lacaux, C., Boone, A., Liousse, C., Serça, D., Adon, M., Diop, B., Akpo, A., Lavenu, F., Mougin, E., and Timouk, F.: Atmospheric nitrogen budget in Sahelian dry savannas, Atmos. Chem. Phys., 10, 2691–2708, doi:10.5194/acp-10-2691-2010, 2010.

Dunion, J. P. and Velden C. S.: The impact of the Saharan air layer on Atlantic tropical cyclone activity, B. Am. Meteorol. Soc., 85, 353–365, doi:10.1175/BAMS-85-3-353, 2004.

Engelstaedter S., Tegen, I., and Washington R.: North African dust emissions and transport, Earth-Sci. Rev., 79, 73–100, 2006.

Fast, J., Gustafson Jr., W. I., Easter, R. C., Zaveri, R. A., Barnard, J. C., Chapman, E. G., Grell, G. A., and Peckham, S. E.: Evolution of ozone, particulates, and aerosol direct radiative forcing in the vicinity of Houston using a fully coupled meteorology-chemistry-aerosol model, J. Geophys. Res., 111, D21305, doi:10.1029/2005JD006721, 2006.

ACPD
11, 28061–28095, 2011

Grant, D., Fuentes, J. D., Delong, M. S., Chan, S, Joseph, E., Kucera, P., Ndiaye, S. A., and Gaye, A. T.: Ozone transport by mesoscale convective systems in Western Senegal, Atmos. Environ., 42, 7104–7114, 2008.

Grell, G. A., Peckham, S. E., Schmitz, R., McKeen, S. A., Frost, G., Shamarock, W. A., and Eder, B.: Fully coupled "online" chemistry within the WRF model, Atmos. Environ., 39, 6957–6975, 2005.

Guenther, A., Hewitt, N. C., Erickson, D., Fall, R., Geron, C., Graedel, T., Harley, P., Klinger, L., Lerdau M., McKay, W. A., Pierce, T., Scholes, B., Steinbrecher, R., Tallamraju, R., Taylor, J., and Zimmerman, P.: A global model of natural volatile organic compound emissions, J J. Geophys. Res., 100, 8873–8892, 1995.

Ismail, S., Ferrare, R. A., Browell, E. V., Kooi, S. A., Dunion, J. P., Heymsfield, G., Notari, A., Butler, C. F., Burton, S., Fenn, M., Krishnamurti, T. N., Biswas, M. K., Chen, G., and Anderson, B.: LASE measurements of water vapor, aerosols and cloud distributions in Saharan air layers and tropical disturbances, J. Atmos. Sci., 67, 1026–1047, 2010.

Jacob, D. J.: Heterogeneous chemistry and tropospheric ozone, Atmos. Environ., 24, 2131–2159, 2000.

Jaeglé, L., Martain, R. V., Chance, K., Steinberger, L., Kurosu, T. P, Jacob, D. J., Modi, A. I., Yoboue, V., Sigha-Nkamdjou, L., and Galy-Lacaux ,C.: Satellite mapping of rain-induced nitric oxide emissions from soils, J. Geophys. Res., 109, D21310, doi:10.1029/2004JD004787, 2004.

Jenkins, G. S., Pratt, A., and Heymsfield, A.: Possible linkages between Saharan dust and tropical cyclone rain band invigoration in Eastern Atlantic during NAMMA-06, Geophys. Res. Lett., 35, L08815, doi:10.1029/2008GL034072, 2008a.

Jenkins, G. S., Camara, M., Ndiaye, S.: Observational evidence of enhanced middle/upper tropospheric ozone via convective processes over the Equatorial Tropical Atlantic during the summer of 2006, Geophys. Res. Lett., 35, L12806, doi:10.1029/2008GL033954, 2008b.

Middleton, N. J. and Goudie, A. S.: Saharan dust: sources and trajectories, T. I. Brit. Geogr., 26, 165–181, 2001.

Myhre, G., Grini, A., Haywood, J. M., Stordal, F. , Chatenet, B. Tanré, D. Sundet, J. K., and Isaksen, I. S. A.: Modeling the radiative impact of mineral dust during the Saharan Dust Experiment (SHADE) campaign, J. Geophys. Res., 108, 8579, doi:10.1029/2002JD002566, 2003.

Real, E., Orlandi, E., Law, K. S., Fierli, F., Josset, D., Cairo, F., Schlager, H., Borrmann, S.,

ACPD

11, 28061–28095, 2011

Kunkel, D., Volk, C. M., McQuaid, J. B., Stewart, D. J., Lee, J., Lewis, A. C., Hopkins, J. R., Ravegnani, F., Ulanovski, A., and Liousse, C.: Cross-hemispheric transport of central African biomass burning pollutants: implications for downwind ozone production, Atmos. Chem. Phys., 10, 3027–3046, doi:10.5194/acp-10-3027-2010, 2010.

Redelsperger, J. L., Thorncroft, C. D., Diedhiou, A., Lebel, T., Parker, D. J., and Polcher, J.: African monsoon multidisciplinary analysis: an international research project and field campaign, B. Am. Meteorol. Soc., 87, 1739–1746, 2006.

Reeves, C. E., Formenti, P., Afif, C., Ancellet, G., Attié, J.-L., Bechara, J., Borbon, A., Cairo, F., Coe, H., Crumeyrolle, S., Fierli, F., Flamant, C., Gomes, L., Hamburger, T., Jambert, C., Law, K. S., Mari, C., Jones, R. L., Matsuki, A., Mead, M. I., Methven, J., Mills, G. P., Minikin, A., Murphy, J. G., Nielsen, J. K., Oram, D. E., Parker, D. J., Richter, A., Schlager, H., Schwarzenboeck, A., and Thouret, V.: Chemical and aerosol characterisation of the troposphere over West Africa during the monsoon period as part of AMMA, Atmos. Chem. Phys., 10, 7575–7601, doi:10.5194/acp-10-7575-2010, 2010.

Rhome, J. R.: Tropical Cyclone Report Hurricane Bertha (AL022008), National Hurricane Center, available at: http://www.nhc.noaa.gov/2008atlan.shtml, 2008.

Saunois, M., Reeves, C. E., Mari, C. H., Murphy, J. G., Stewart, D. J., Mills, G. P., Oram, D. E., and Purvis, R. M.: Factors controlling the distribution of ozone in the West African lower troposphere during the AMMA (African Monsoon Multidisciplinary Analysis) wet season campaign, Atmos. Chem. Phys., 9, 6135–6155, doi:10.5194/acp-9-6135-2009, 2009.

Stewart, D. J., Taylor, C. M., Reeves, C. E., and McQuaid, J. B.: Biogenic nitrogen oxide emissions from soils: impact on NO_x and ozone over west Africa during AMMA (African Monsoon Multidisciplinary Analysis): observational study, Atmos. Chem. Phys., 8, 2285–2297, doi:10.5194/acp-8-2285-2008, 2008.

Tang, Y., Carmichael, G. R., Kurata, G., Uno, I., Weber, R. J., Song, C.-H., Guttikunda, S. K., Woo, J.-H., Streets, D. G., Wei, C., Clark A. D., Huebert, B., and Anderson, T. L.: Impacts of dust on regional tropospheric chemistry during the ACE-Asia experiment: a model study with observations, J. Geophys. Res., 109, D19S21, doi:10.1029/2003JD003806, 2004.

Thompson, A. M., Witte, J. C., McPeters, R. D., Oltsman, S. J., Schmidlin, F. J., Logan, J. A. Fujiwara, M., Kirchhoff, V. W. J. H., Posny, F., Coetzee, G. J. R., Hoegger, B., Kawakami, S., Ogawa, T., Johnson, B. J., Vömel, H., and Labow, G.: Southern Hemisphere Additional Ozonesondes (SHADOZ) 1998–2000 tropical ozone climatology 1. Comparison with Total Ozone Mapping Spectrometer (TOMS) and ground-based measurements, J. Geophys. Res.,

ACPD
11, 28061–28095, 2011

108, 8238, doi:10.1029/2001JD000967, 2003.
Thouret, V., Saunois, M., Minga, A., Mariscal, A., Sauvage, B., Solete, A., Agbangla, D., Nédélec, P., Mari, C., Reeves, C. E., and Schlager, H.: An overview of two years of ozone radio soundings over Cotonou as part of AMMA, Atmos. Chem. Phys., 9, 6157–6174, doi:10.5194/acp-9-6157-2009, 2009.
Twohy, C. H., Kreidenweis, S. M., Eidhammer, T., Browell, E. V., Heymsfield, A. J., Bansemer, A. R., Anderson, B. E., Chen, G., Ismail, S., Demott, P. J., and Van Den Heever, S. C.: Saharan dust particles nucleate droplets in Eastern Atlantic clouds, Geophys. Res. Lett., 36, L01807, doi:10.1029/2008GL035846, 2009.
Van der A, R. J., Eskes, H. J. , Boersma, K. F., van Noije, T. P. C., Van Roozendael, M., De Smedt, I., Peters,D. H. M. U., and Meijer, E. W.: Trends, seasonal variability and dominant NO_x source derived from a ten year record of NO_2 measured from space, J. Geophys. Res., 113, D04302, doi:10.1029/2007JD009021, 2008.
Vlasenko, A., Sjogren, S., Weingartner, E., Stemmler, K., Gäggeler, H. W., and Ammann, M.: Effect of humidity on nitric acid uptake to mineral dust aerosol particles, Atmos. Chem. Phys., 6, 2147–2160, doi:10.5194/acp-6-2147-2006, 2006.
Williams, J. E., Scheele, M. P., van Velthoven, P. F. J., Cammas, J.-P., Thouret, V., Galy-Lacaux, C., and Volz-Thomas, A.: The influence of biogenic emissions from Africa on tropical tropospheric ozone during 2006: a global modeling study, Atmos. Chem. Phys., 9, 5729–5749, doi:10.5194/acp-9-5729-2009, 2009.
Zhang, Y., Sunwoo, Y., Kotamarthi, V., Carmichael, G. R.: Photochemical oxidant processes in the presence of dust: an evaluation of the impact of dust on particulate nitrate and ozone formation, J. Appl. Meteorol., 33, 813–824, 1994.
Ziemke, J. R., Chandra, S., Duncan, B. N., Froidevaux, L., Bhartia, P. K., Levelt, P. F., and Waters, J. W.: Tropospheric ozone determined from Aura OMI and MLS: evaluation of measurements and comparison with the global modeling initiative's chemical transport model, J. Geophys. Res., 111, D19303, doi:10.1029/2006JD007089, 2006.
Zipser, E. J., Twohy, C. H., Tsay, S. C., Thornhill, K. L., Tanelli, S., Ross, R., Krishnamurti, T. N., Ji, Q., Jenkins, G., Ismail, S., Hsu, N. C., Hood, R., Heymsfield, G. M., Heymsfield, A., Halverson, J., Goodman, H. M., Ferrare, R., Dunion, J. P., Douglas, M., Cifelli, R., Chen, G., Browell, E. V., and Anderson, B.: The Saharan air layer and the fate of African Easterly Waves – NASA's AMMA field study of tropical cyclogenesis, B. Am. Meteorol. Soc., 90, 1137–1156, 2009.

ACPD
11, 28061–28095, 2011

Table 1. Surface 925–550 hPa Column O_3, Relative humidity and OMI AI index.

Date (2008)	Time (UTC)	O_3 925–550 hPa (DU)	RH 925–550 hPa (%)	OMI AI (13–16° N, 16–19° W)
8 Jun	12:00	6.6	32.2	2.11
10 Jun	12:00	7.4	37.3	1.29
12 Jun	12:00	20.5	65.1	
15 Jun	12:00	11.3	28.7	2.02
26 Jun	12:00	10.5	37.2	1.98
2 Jul	12:00	14.2	67.3	
2 Aug	12:00	10.3	31.3	3.80
27 Aug	12:00	6.4	88.5	0.58
3 Sep	12:00	11.0	68.8	0.61

ACPD
11, 28061–28095, 2011

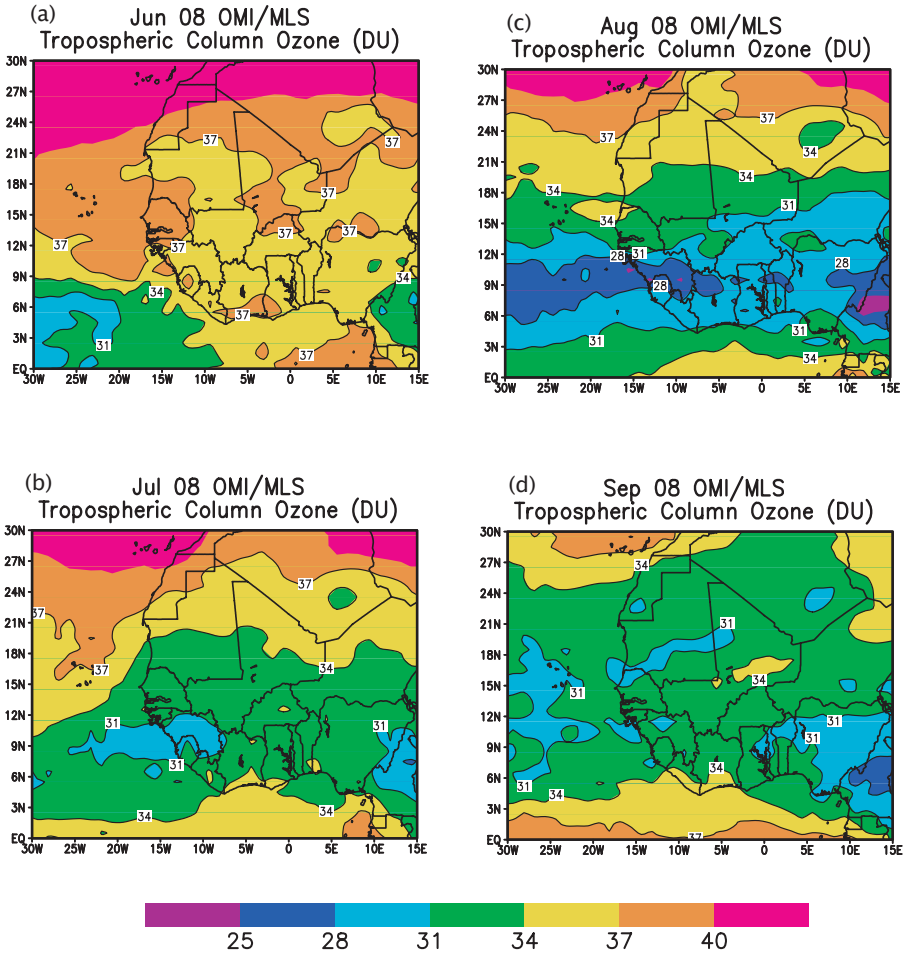

Fig. 1. OMI/MLS Total Column Ozone for **(a)** June 2008; **(b)** July 2008; **(c)** August 2008; **(d)** September 2008. Units are in DU.

ACPD
11, 28061–28095, 2011

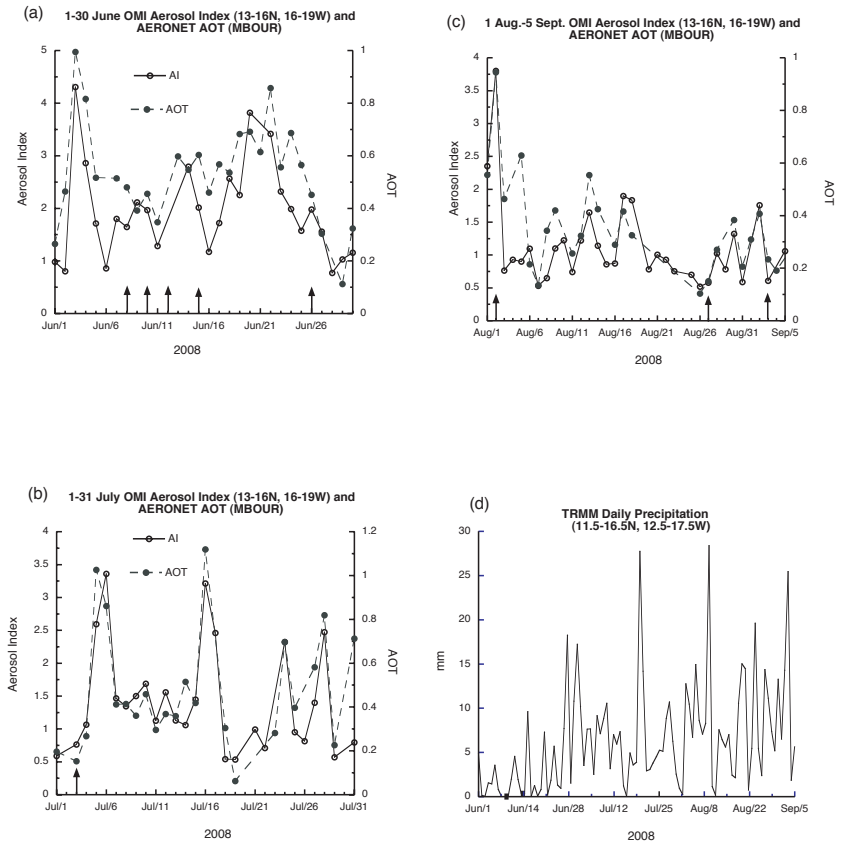

Fig. 2. Daily area averaged (13–16° N, 16–19° W) OMI derived Aerosol Index (AI) and Mbour, Senegal AOT for: **(a)** June; **(b)** July; **(c)** 1 August–5 September; **(d)** Area averaged (11.5–16.5° N, 12.5–17.5° W) TRMM daily averaged precipitation for 1 June–5 September 2006. Arrows represent launch ozonesonde launch dates.

ACPD
11, 28061–28095, 2011

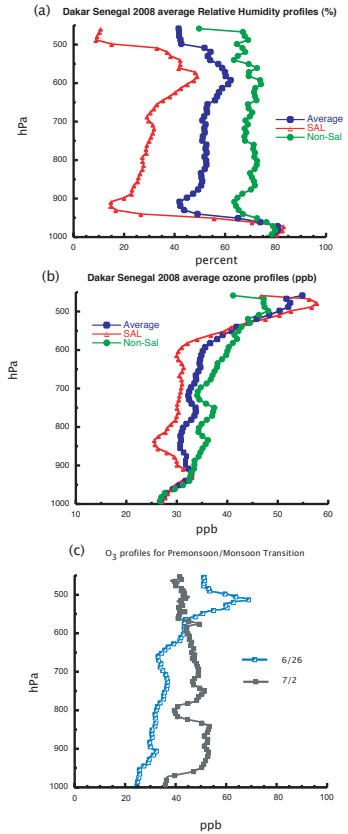

Fig. 3. (a) 1000–450 hPa observed lower/middle tropospheric average vertical profiles for SAL, Non-SAL and the average of all ozonesondes during the summer of 2008 for: **(a)** relative humidity (percent); **(b)** ozone (ppb). **(c)** Vertical profile of ozone (ppb) for the pre-monsoon/monsoon transition on 26 June and 2 July. Units are ppb.

ACPD
11, 28061–28095, 2011

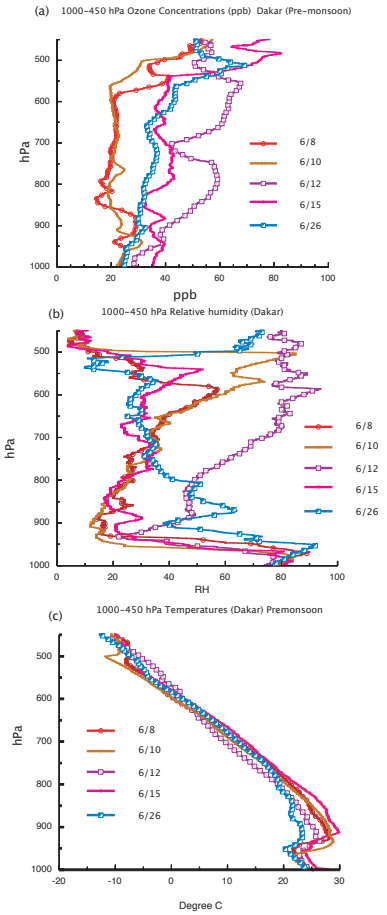

Fig. 4. 1000–450 hPa lower/middle tropospheric vertical profiles of: **(a)** O_3 concentrations; **(b)** relative humidity and **(c)** temperature for the pre-monsoon period.

ACPD
11, 28061–28095, 2011

Enhancement and depletion of lower/middle tropospheric ozone

G. S. Jenkins et al.

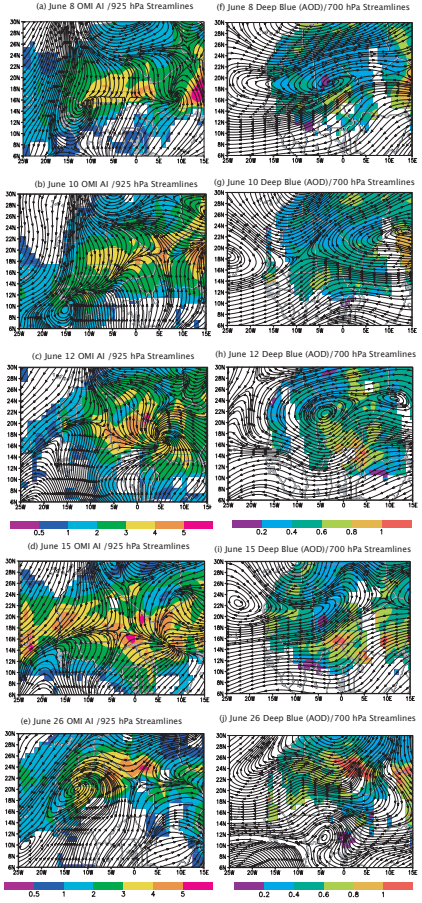

Fig. 5. Pre-Monsoon OMI AI and 925 hPa streamlines (**a**–**e**): Deep Blue AOT and 700 hPa streamlines (**f**–**j**): (**a** and **f**) 8 June; (**b** and **g**); 10 June; (**c** and **h**) 12 June; (**d** and **i**) 15 June; (**e** and **j**) 26 June.

ACPD
11, 28061–28095, 2011

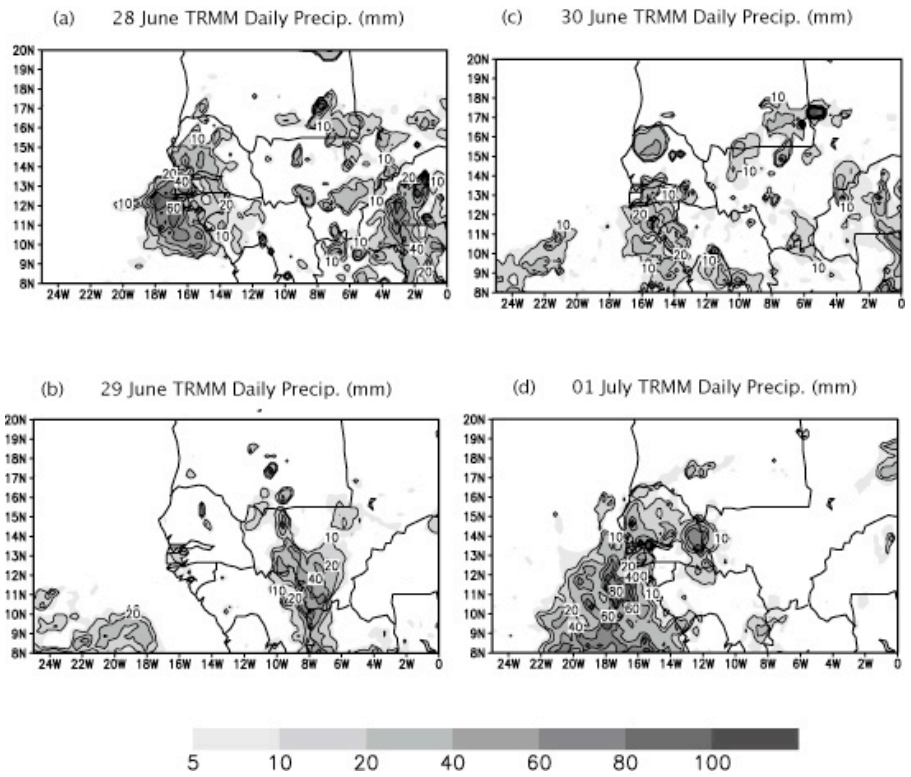

Fig. 6. TRMM daily Precipitation amounts **(a)** 28 June; **(b)** 29 June; **(c)** 30 June; **(d)** 1 July. Units are mm.

ACPD
11, 28061–28095, 2011

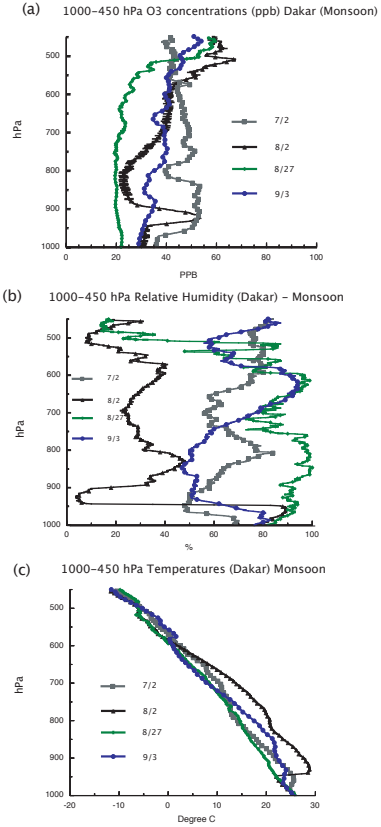

Fig. 7. 1000–450 hPa lower/middle tropospheric vertical profiles of: **(a)** O_3 concentrations; **(b)** relative humidity and **(c)** temperature for the monsoon period.

ACPD
11, 28061–28095, 2011

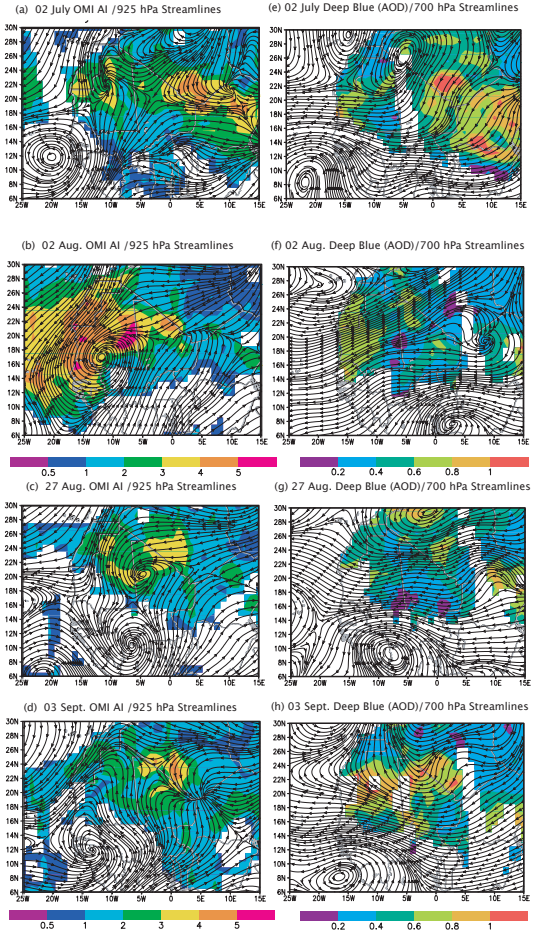

Fig. 8. Monsoon OMI AI/925 hPa streamlines (panels **a**–**d**) and Deep Blue AOT/700 hPa streamlines (panels **e**–**h**): (**a** and **e**) 2 July; (**b** and **f**); 2 August; (**c** and **g**) 27 August; (**d** and **h**) 3 September.

ACPD
11, 28061–28095, 2011

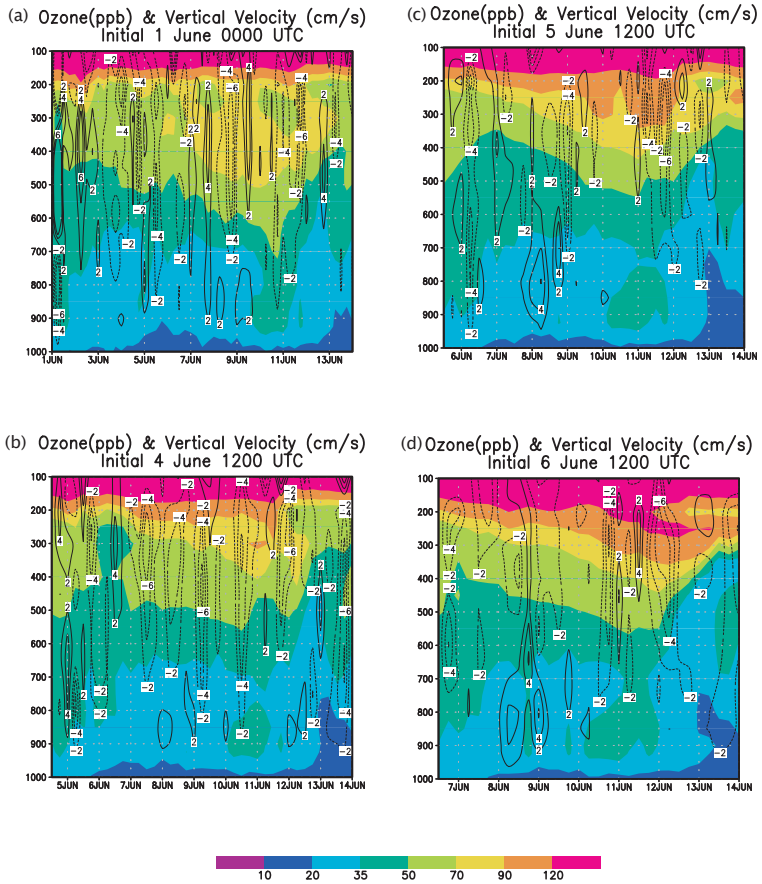

Fig. 9. Time-height profiles of O_3 concentrations and vertical velocity at 14.5° N, 17.5° W for initial conditions beginning at: **(a)** 1 June 00:00 UTC; **(b)** 4 June 12:00 UTC; **(c)** 5 June 12:00 UTC; **(d)** 6 June 12:00 UTC. Units in ppb and cm s^{-1}.

ACPD
11, 28061–28095, 2011

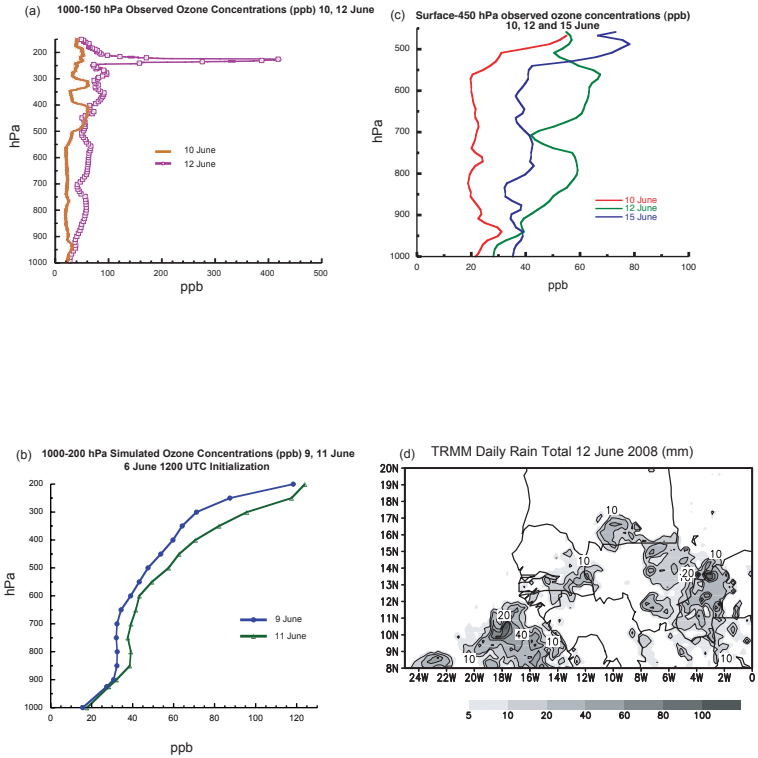

Fig. 10. **(a)** Surface-450 hPa averaged vertical profile of O_3 concentrations fur 10, 12, 15; **(b)** June 1000–150 hPa observed vertical profile of O_3 at Dakar for 10,12 June, 12:00 UTC; **(c)**1000–200 hPa WRF-CHEM vertical profile of O_3. Units in ppb. **(d)** TRMM 12 July total rain (mm).

ACPD
11, 28061–28095, 2011

Enhancement and depletion of lower/middle tropospheric ozone

G. S. Jenkins et al.

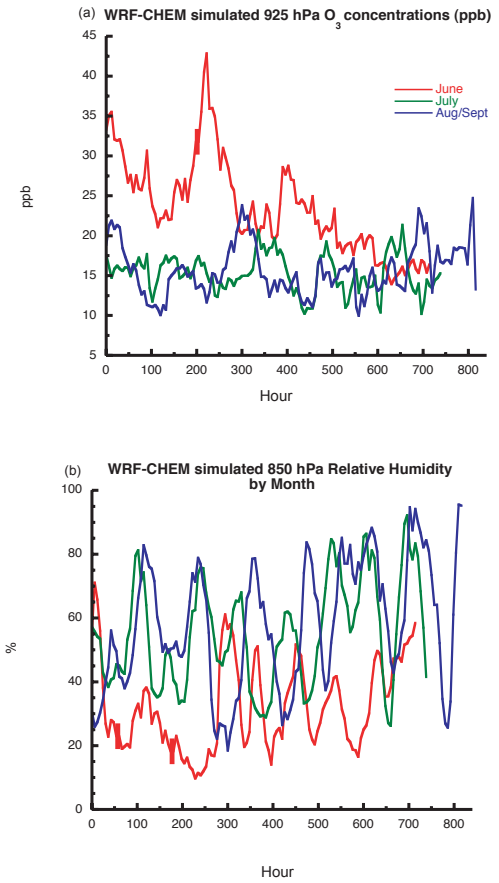

Fig. 11. WRF-Chem simulation of: **(a)** 925 hPa O_3 concentrations for June, July and August; **(b)** 850 hPa relative humidity for June, July and August. Units are ppb for O_3, % for RH and ˚C for temperature.

ACPD
11, 28061–28095, 2011

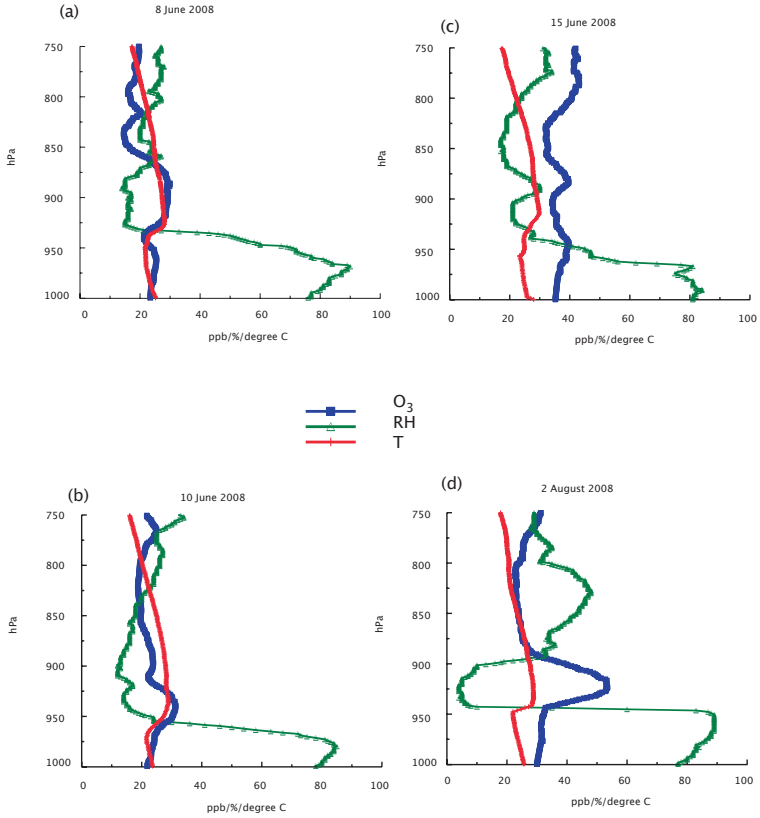

Fig. 12. 1000–750 hPa vertical profiles of O_3 (blue), RH (green) and Temperature (red) for identified SAL events. **(a)** 8 June; **(b)** 10 June; **(c)** 15 June; **(d)** 2 August. Units are ppb for O_3, % for RH and ˚C for temperature.

ACPD
11, 28061–28095, 2011

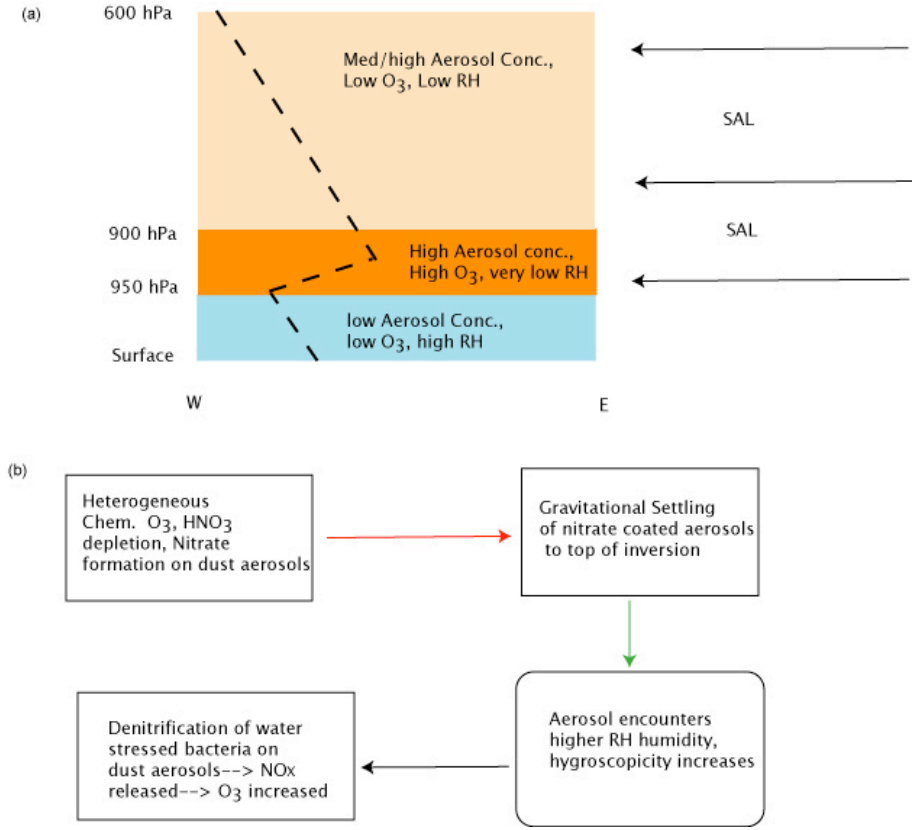

Fig. 13. **(a)** A depiction of relative humidity, aerosol and O_3 concentrations in various layer of the lower/middle troposphere associated with a SAL intrusion. The dash line represents the vertical profile of temperature. **(b)** Proposed mechanism for increasing O_3 in the 950–900 hPa layer.

ACPD
11, 28061–28095, 2011